Non-linear flow law of rockglacier creep determined from geomorphological observations: A case study from the Murtèl rockglacier (Engadin, SE Switzerland)

Marcel Frehner[1], Dominik Amschwand[1] and Isabelle Gärtner-Roer[2]
[1]Geological Institute, ETH Zurich, Switzerland, marcel.frehner@erdw.ethz.ch
[2]Department of Geography, University of Zurich, Switzerland

Introduction

The creep behavior (i.e., rheology) of rockglaciers may deviate from the well-known flow-law for pure ice. Here we aim at constraining the non-linear viscous flow law governing rockglacier creep based on geomorphological criteria and borehole deformation data. As a case study we use the Murtèl rockglacier (upper Engadin valley, SE Switzerland) for which high-resolution digital elevation models (DEM), time-lapse borehole deformation data, and geophysical soundings exist that reveal the exterior and interior architecture and dynamics of the landform.

Rockglaciers often feature a prominent furrow-and-ridge topography. For the Murtèl rockglacier, Frehner et al. (2015) reproduced the wavelength, amplitude, and distribution of the furrow-and-ridge morphology using a linear viscous (Newtonian) flow model. Arenson et al. (2002) presented borehole deformation data, which highlight the basal shear zone at about 30 m depth and a curved deformation profile above the shear zone. Similarly, the furrow-and-ridge morphology also exhibits a curved geometry in map view. Hence, the surface morphology and the borehole deformation data together describe a curved 3D geometry, which is close to, but not quite parabolic.

Linear viscous models result in perfectly parabolic flow geometries; non-linear creep leads to localized deformation at the sides and bottom of the rockglacier while the deformation in the interior and top are less intense. In other words, non-linear creep results in non-parabolic flow geometries. By comparing the measured curved 3D geometry with theoretical 3D flow geometries, we determine the most adequate flow-law that fits the natural deformation geometry best.

The Murtèl rockglacier

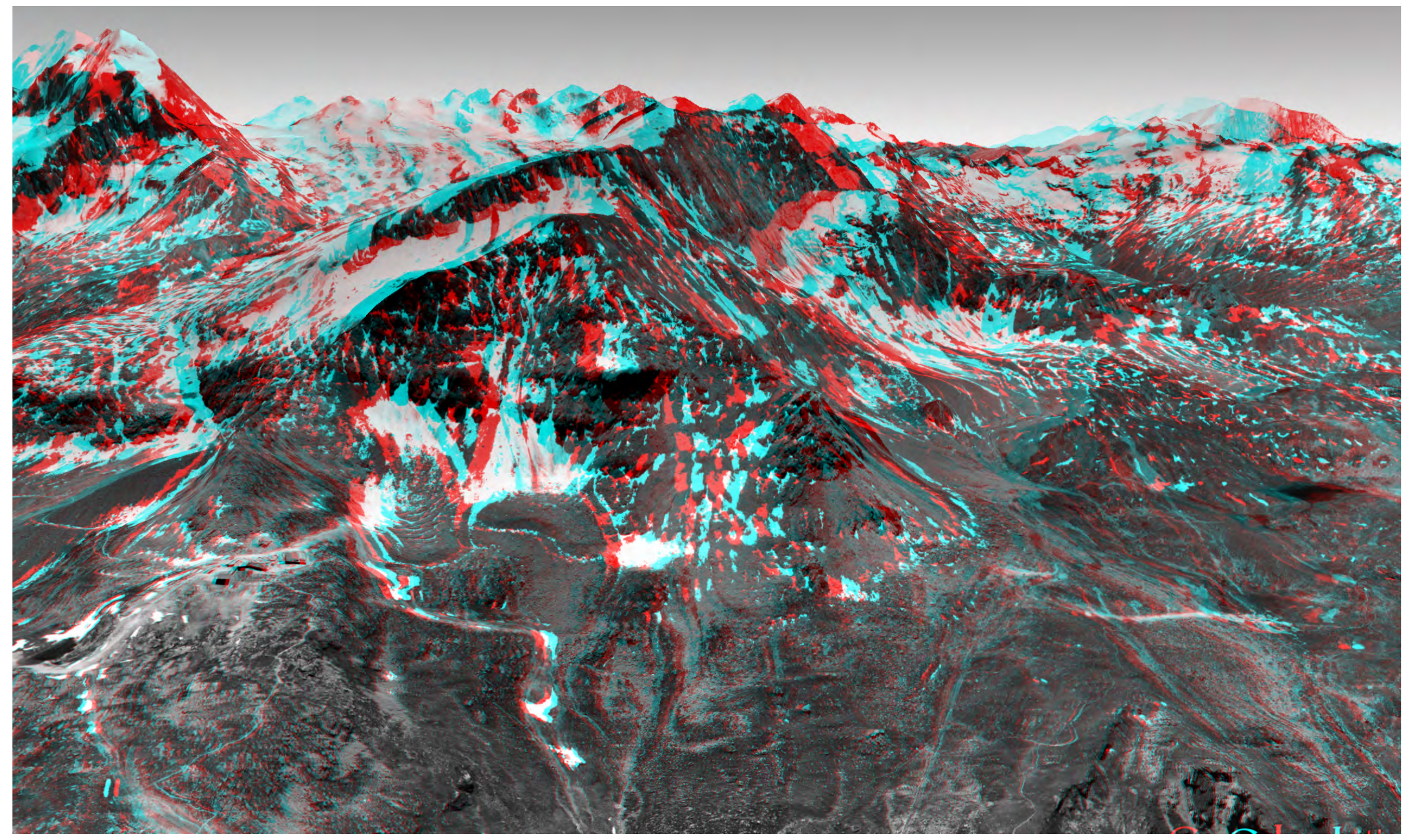

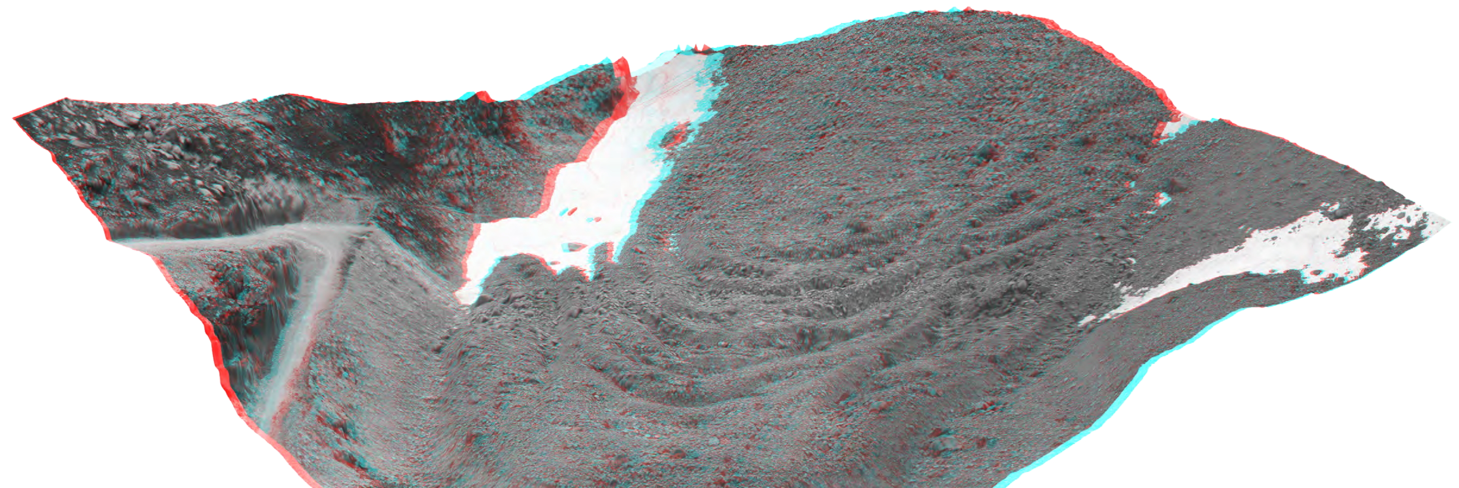

↖ *Fig. 2: High-resolution (8 cm) DEM and color information of the Murtèl rockglacier (courtesy of J. Müller).*

← *Fig. 1: Regional overview (Google Earth) of Piz Corvatsch and the Murtèl cirque.*

How to view the 3D images:
Grab a pair of red-blue 3D glasses. Important: Relax your eyes; e.g. focus on the furthest peaks in Fig. 1.

Motivation: Our previous work

In Frehner et al. (2015), we applied the buckle folding theory for linear viscous (Newtonian) materials to explain the furrow-and-ridge morphology on the Murtèl rockglacier.

Buckle folding theory in a nutshell
Buckle folding is the mechanical response of layered viscous materials to layer-parallel compression. The wavelength (L) depends on the viscosity ratio (R) between the stiff (folded) and soft layer and on the thickness of the stiff layer (h).

Based on the spacing of the furrows and ridges (L≈20 m) we determined the effective (Newtonian) viscosity ratio between the upper layer (h=3 m) and the main rockglacier body as R=21.

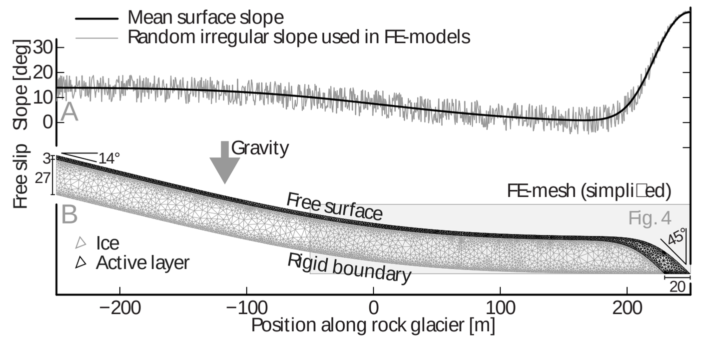

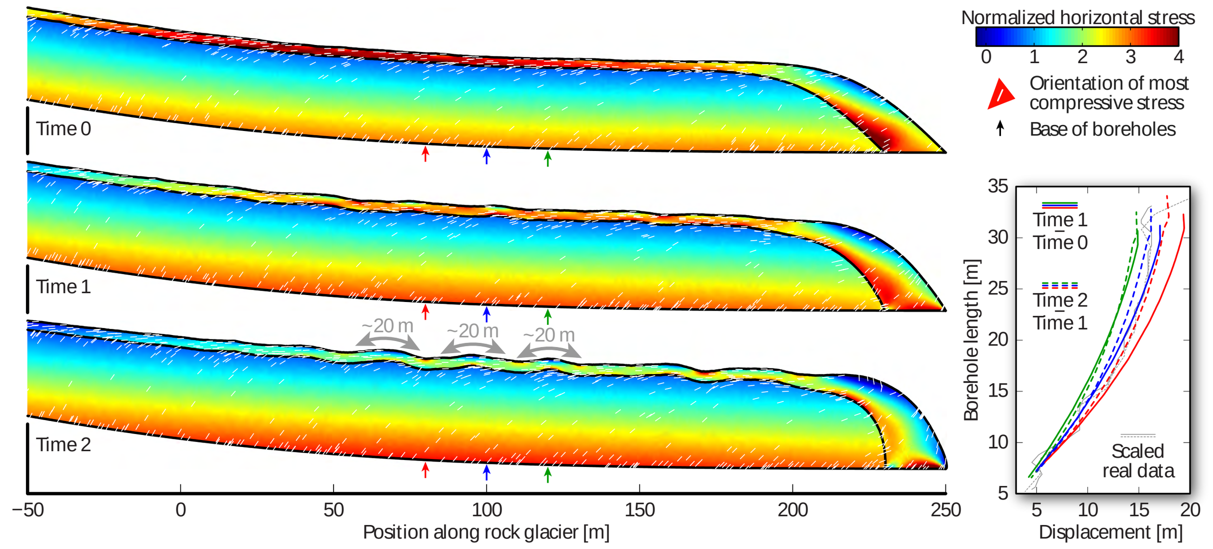

↑ *Fig. 3: 2D linear viscous finite-element model based on Murtèl rockglacier (h=3 m, R=21).*
→ *Fig. 4: The simulation reproduces Murtèl's furrow-and-ridge morphology (L≈20 m) and the upper part of the borehole deformation.*

Basic research idea

Flow of linear viscous (Newtonian) materials leads to perfectly parabolic flow structures; flow of non-linear viscous materials leads to curved, but not parabolic flow structures. Ideally, the **power-law exponent of the curved flow structures** (m) is **one larger than** the **power-law stress exponent of the non-linear rheological flow law** (n) (Table 1).

	Rheological flow law (Glen's (1952) flow law)	Geometry of furrow-and-ridge morphology	Horizontal borehole deformation with depth
General:	$\tau^n = A\dot{\varepsilon}$	$u_x(x) = Bx^{n+1} = Bx^m$	$u_x(z) = Cz^{n+1} = Cz^m$
Newtonian:	$\tau = A\dot{\varepsilon}$	$u_x(x) = Bx^{1+1} = Bx^2$	$u_x(z) = Cz^{1+1} = Cz^2$

↑ *Table 1: Relationship between rheological flow law and ideal flow geometries. τ: stress, $\dot{\varepsilon}$: strain rate, u_x: displacement in flow direction, n: power-law exponent of rheological flow law, m: power-law exponent of flow structure, A, B, C: material or geometrical constants.*

In principle, **geometrical analysis** of flow structures on/within a rockglacier should allow **determinining the power-law exponent** (n) that governs the viscous flow.

Used data

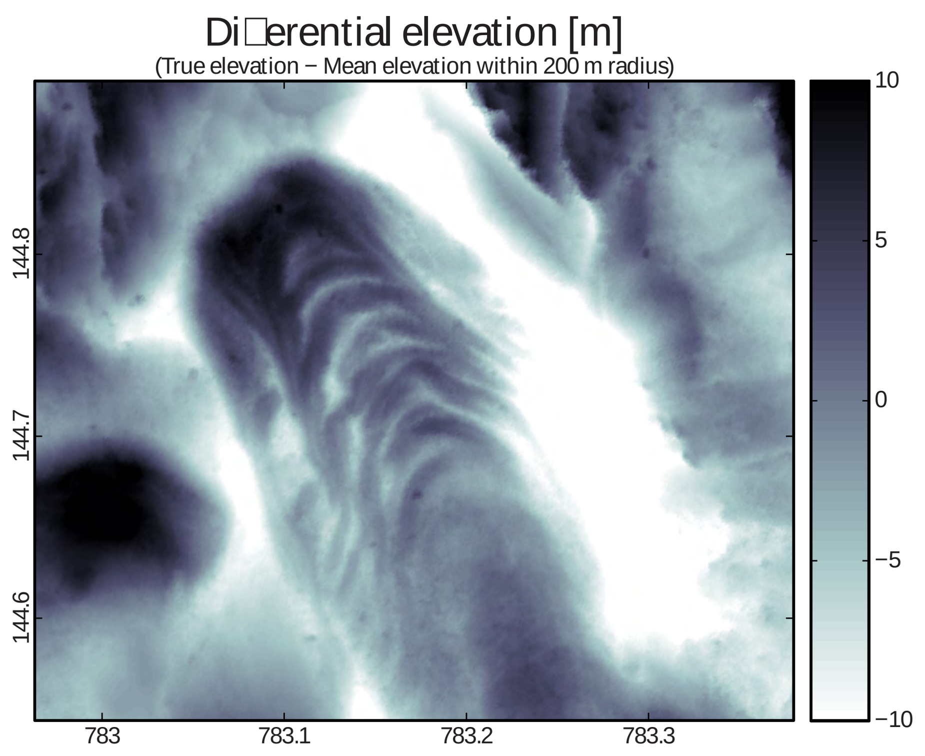

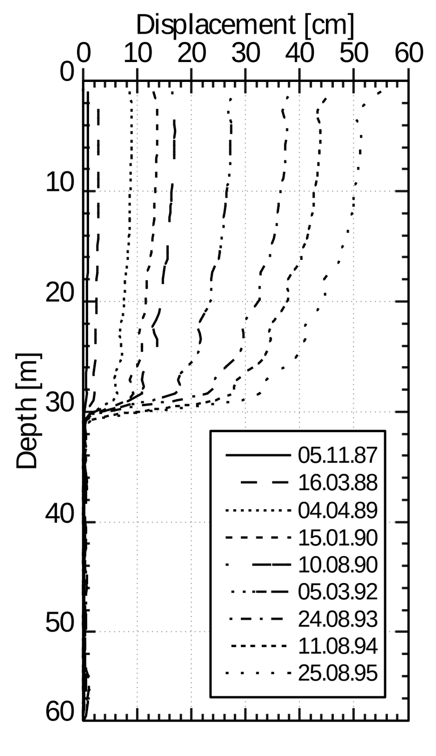

↑ *Fig. 5: Differential elevation calculated from a 1 m resolution digital elevation model (Frehner et al., 2015).*

↑ *Fig. 6: Borehole deformation (Arenson et al., 2002).*

Workflow

Using the **curved furrow-and-ridge morphology** in map view (Fig. 5) and the **curved borehole deformation data** in a vertical view (Fig. 6), we apply the following workflow:

① Digitize the curved flow structures, both in map view and in vertical direction.

② **Find the power-law function** that best fits the curved geometry. Various assumptions and boundary conditions may be applied:
- Part that is considered: entire structure, reject few meters on each side in map view, reject the top 5 m and/or bottom few meters (shear zone) in borehole data
- Fixed value at the end of the structure
- Fixed gradient at the top of the borehole

③ From the best-fitting geometrical power-law exponent (m), infer the power-law stress exponent of the rheological flow law (n).

First results for borehole data

So far, we analyzed two borehole curves (Fig. 7 & 8, Table 1). Considering the **entire borehole**, the **power-law fit performs significantly better** (R^2>0.92) **than the quadratic fit** (R^2<0.75) and we find **power-law exponents of 5.14>m>7.30**. Considering **only the middle section** of the borehole, all different fitting curves perform equally well (R^2>0.96) and we find **power-low exponent close to m=2.**

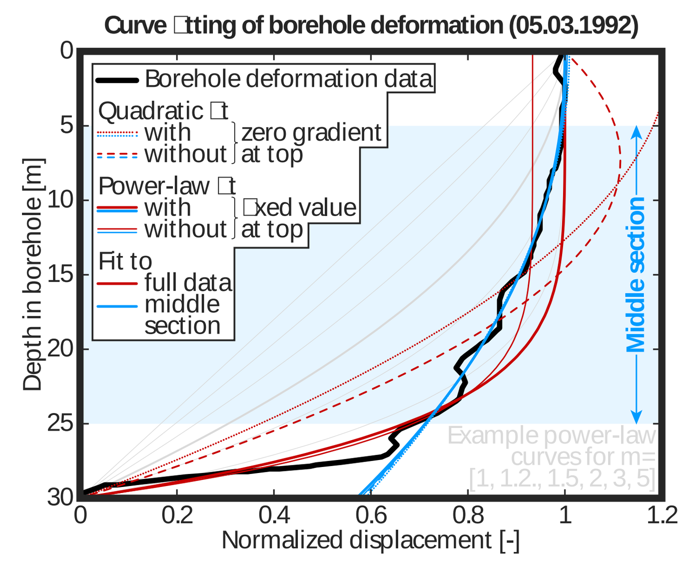

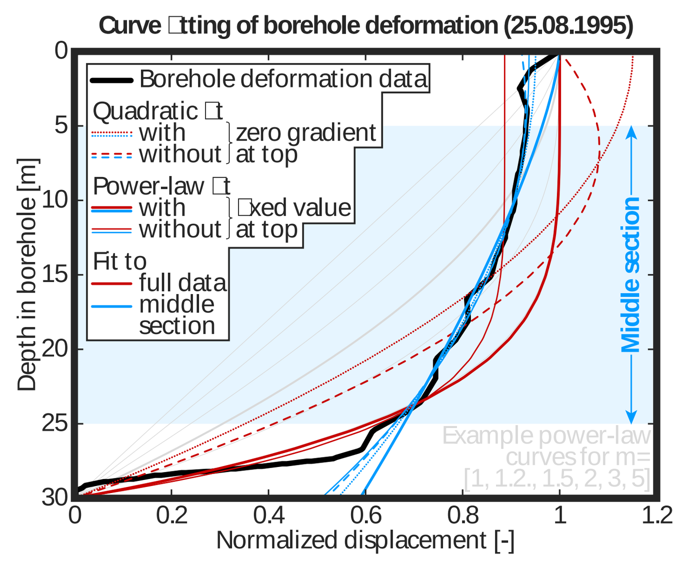

		Quadratic fit						Power-law fit			
Fit to entire borehole		✓	✓	✓				✓	✓		
Fit only to middle section					✓	✓	✓			✓	✓
Fixed bottom [d(30 m) = 0]		✓	✓	✓				✓	✓		
Fixed top [d(0 m) = 1]		✓		✓			✓	✓		✓	
Zero gradient at top [dd(0 m)/dz = 0]			✓	✓		✓	✓	✓	✓	✓	✓
Symbol in Fig. 7 & 8											
05.03.	m=	2 (forced)						6.06	7.30	2.19	2.10
1992	R^2=	0.71	0.58	0.38	0.98	0.98	0.98	0.94	0.96	0.98	0.98
25.08.	m=	2 (forced)						5.14	6.75	1.36	2.37
1995	R^2=	0.75	0.67	0.60	0.99	0.98	0.87	0.92	0.96	0.96	0.99

↖ *Fig. 7 & ↑ Fig. 8: Borehole deformation curves (Arenson et al., 2002) and fitting functions using different conditions.*

← *Table 1: Curve fitting details. Best fits are obtained using power-law functions and fitting only the middle section of the borehole.*

Discussion, Conclusions & Outlook

Preliminary results suggest that the flow law governing deformation of the Murtèl rockglacier has a **power-law stress exponent (n) between 4 and 6** (i.e., m–1). However, the rockglacier may be **divided into a lower part** with strong strain localization (**shear zone**) and the **main rockglacier body** with an almost **linear (n=1) rheological flow law.**

Outlook
Our work continues during the BSc Thesis of D. Amschwand. Next, we will analyze the furrow-and-ridge morphology in a similar way as the borehole deformation data. Subsequently, we will feed the best-fitting rheological flow law into a 3D finite-element model (Fig. 9) to study the internal dynamics (stresses & strain rates) of rockglacier flow. Expect new results at ICOP (20–24 June 2016, Postdam).

↙ *Fig. 9: Different views of 3D feasibility simulation. A DEM (Fig. 2) defines the model topography. The base is equal to the 2D model (Fig. 3).*

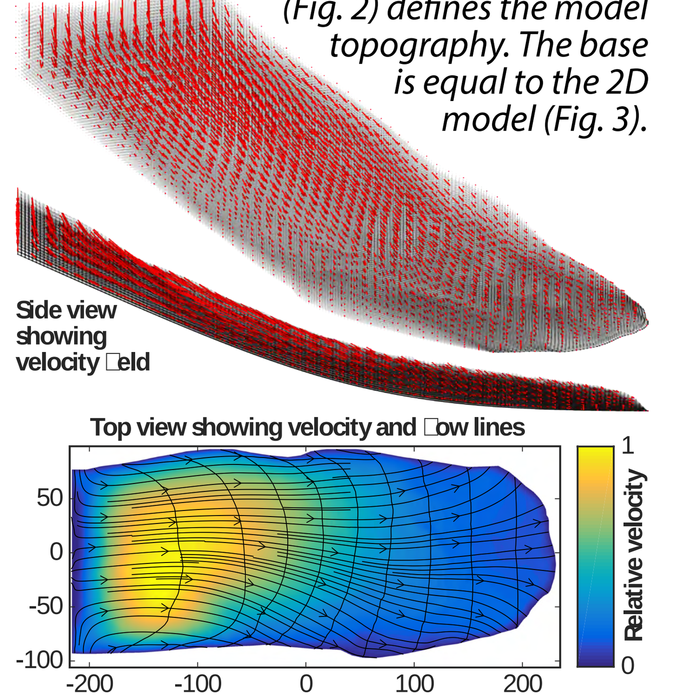

References
Arenson L., Hoelzle M. and Springman S., 2002: Borehole deformation measurements and internal structure of some rock glaciers in Switzerland. Permafrost and Periglacial Processes 13, 117–135.
Frehner M., Ling A.H.M. and Gärtner-Roer I., 2015: Furrow-and-ridge morphology on rockglaciers explained by gravity-driven buckle folding: A case study from the Murtèl rockglacier (Switzerland), Permafrost and Periglacial Processes 26, 57–66.
Glen J.W., 1952: Experiments on the deformation of ice. Journal of Glaciology 2, 111–114.